

C–H···O Hydrogen Bond between *N*-Methyl Maleimide and Dimethyl Sulfoxide: A Combined NMR and Ab Initio Study

Bing Wang,[†] James F. Hinton, and Peter Pulay*

Department of Chemistry and Biochemistry, University of Arkansas, Fayetteville, Arkansas 72701

Received: September 12, 2002; In Final Form: February 24, 2003

The proton chemical shifts in *N*-methyl maleimide (NMM) in dry dimethyl sulfoxide-*d*₆ (DMSO) and in cyclohexane-*d*₁₂ solutions have been measured between 30 and 70 °C. The proton shieldings have also been calculated using the gauge-including atomic orbital method at the Hartree–Fock and hybrid Becke–Lee–Yang–Parr (B3LYP) density functional levels, using the 6-311++G and 6-311++G** basis sets. There is a 0.4 ppm discrepancy between the observed chemical shift of the ring protons in DMSO solution and the value derived from the calculations, whereas only 0.1 ppm or less is expected (see Wang, B.; Hinton, J. F.; Pulay, P. *J. Comput. Chem.* **2002**, *23*, 492). The discrepancy almost certainly arises from a C–H···O hydrogen bond between the acidic ring proton and the oxygen of DMSO. This is supported by its strong temperature coefficient and by model calculations on NMM–DMSO, NMM–acetone, and NMM–water complexes at the B3LYP and second-order Møller–Plesset levels with large basis sets (up to 6-311++G(3df,3pd)). The latter predict bonding strengths of 3–4 kcal/mol, large for a C–H···O hydrogen bond. The sign and approximate magnitude of the effect of hydrogen bonding on the ring proton chemical shift agree with the calculations.

1. Introduction

There has been increasing interest in C–H···O hydrogen bonds recently, both experimentally and theoretically.^{1–3} Because carbon is not particularly electronegative, the ability of the C–H group to serve as a proton donor in hydrogen bonding depends on the carbon hybridization (C(sp)–H > C(sp²)–H > C(sp³)–H) and on the electron-withdrawing strength of adjacent substituents.^{4–6} Although the C–H···O interaction energy varies between 0.5 and 2 kcal/mol⁷ and is thus much weaker than conventional hydrogen bonds, it can play an important role in molecular conformation,⁸ crystal packing,⁹ and protein folding.¹⁰ Close C–H···O contacts have been observed widely in high-resolution protein structures. The most frequently occurring C–H···O hydrogen bonds are those in which the C^α–H group acts as donor, and the carbonyl oxygen in a neighboring β-sheet peptide strand acts as acceptor (see Figure 1). Bifurcated hydrogen bonding patterns have also been observed in α-helix structures and in a collagen triple helix¹¹ (see Figure 1). Dixon et al.¹² obtained about 3.0 kcal/mol for the C^α–H···O=C hydrogen bond energy in *N,N*-dimethylformamide dimers at the second-order Møller–Plesset (MP2) theory¹³ with the aug-cc-pVTZ basis set.^{14,15} The hydrogen bond involving the C^α–H group at the charged lysine residue was found to be even stronger than a conventional O–H···O interaction.¹⁶ These studies indicate that this weak hydrogen bond can contribute significantly in the determination of protein conformation. Surprisingly, no existing protein force field takes this effect into account to our knowledge.

Traditionally, infrared (IR) spectroscopy was the leading method for the identification of hydrogen bonds.¹⁷ For instance, the formation of an O–H···O hydrogen bond elongates and weakens the O–H bond. The resulting red shift of the O–H

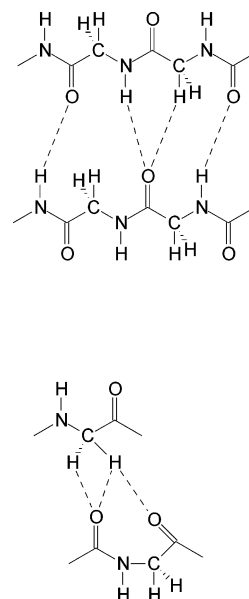


Figure 1. C–H···O interactions in protein β-sheets (top) and in the collagen triple helix (bottom).

bond stretching frequency can be easily detected in the IR spectra, and its magnitude indicates the strength of the hydrogen bond. For the C–H···O hydrogen bond, this method is not applicable because experimental¹⁸ and theoretical³ evidence indicates that hydrogen bonding changes the C–H bond length very little and in some cases even shortens it, leading to the blue shift of C–H bond stretching frequency. This phenomenon was named anti-hydrogen bond.^{19,20} However, Scheiner et al.^{3,21} have concluded, from a set of careful calculations, that “anti-hydrogen” bonds do not differ fundamentally from conventional hydrogen bonds. According to their results, the electron density redistribution upon hydrogen bond formation is similar for both the C–H···O and the O–H···O interactions. The amount of

* To whom correspondence should be addressed.

[†] Current address: Department of Chemistry, Pennsylvania State University, University Park, PA 16802.

charge transferred from a donor to an acceptor is roughly proportional to the binding strength.

NMR chemical shifts reflect the electronic structure in a molecule and therefore can be a powerful tool for identifying and characterizing hydrogen bonds. The formation of hydrogen bonds shifts electron density from the proton acceptor to the donor, resulting in deshielding of the bridging hydrogen atom. In conventional hydrogen bonds, the bridging proton chemical shifts are moved downfield by 2–4 ppm. Changes of 1–2 ppm in the C–H proton chemical shift have been observed in a number of cases^{22,23} and taken as evidence for the existence of C–H \cdots O hydrogen bonds. For instance, unusual downfield proton NMR chemical shifts were observed at the C $^{\epsilon 1}$ –H proton of the catalytic histidine in resting α -lytic protease and subtilisin BPN (bacterial proteinase novo) resonates²⁴ and taken as evidence that the C $^{\epsilon 1}$ –H forms a hydrogen bond with a backbone carbonyl oxygen. The frequent occurrence of this weak hydrogen bond at the catalytic center of Asp–His–Ser triads in enzymes indicates functional importance.

There have been ab initio NMR chemical shielding calculations that addressed the nature of the O–H \cdots O hydrogen bond.^{25,26} According to these studies, the shielding component perpendicular to the hydrogen bond axis depends strongly on the length of the hydrogen bond, resulting in a correlation between the isotropic chemical shifts of the bridging proton and the R(O \cdots O) bond length. Calculations by the Scheiner group²⁷ have shown that most of the above conclusions also apply to C–H \cdots O hydrogen bonds.

In our NMR study of peptide analogues, we found a surprising 0.4 ppm difference between the experimental and calculated chemical shifts of the C–H proton of maleimide in dry dimethyl sulfoxide (DMSO) solution. This lies outside the normal range of deviations for other amide molecules (~ 0.1 ppm).²⁸ It may be due to C–H \cdots O hydrogen bonds to the solvent DMSO. To explore this possibility and characterize the nature of this weak interaction, we have performed ab initio calculations and recorded temperature-dependent NMR spectra for *N*-methyl maleimide (NMM), which, by not having an acidic proton, is a better experimental model than maleimide itself. In our previous studies,^{28,29} we have shown that solvent effects on relative chemical shifts largely cancel out, not only in nonpolar solvents²⁹ but also in polar solvents and substrates such as amides DMSO and water.²⁸ For example, we could reproduce the chemical shifts of 18 aliphatic hydrogens in model amides in DMSO and water (D₂O) solutions with a mean absolute deviation below 0.1 ppm by calculations on isolated molecules.²⁸ The results, as expected, are even better in nonpolar solvents. For example, the chemical shifts of aromatic hydrogens in a number of aromatic molecules in CDCl₃ solution are reproduced to a few hundredths of a ppm by calculations on isolated molecules.²⁹ Similar conclusions have been reached earlier by Rablen,³⁰ who used larger sample set but did not remeasure the chemical shifts as we did.

2. Experimental and Computational Details

N-methyl maleimide (NMM) was obtained commercially and used without further purification. DMSO-*d*₆ and cyclohexane-*d*₁₂ were selected as solvents. DMSO is particularly suitable for detecting the C–H \cdots O hydrogen bond because, unlike water, it contains no hydrogen donor. DMSO was carefully dried over molecular sieve before use and handled in a glovebox filled with dry nitrogen. A cyclohexane solution was also prepared because hydrogen bonds cannot form between NMM and cyclohexane. To obtain the temperature dependence of proton

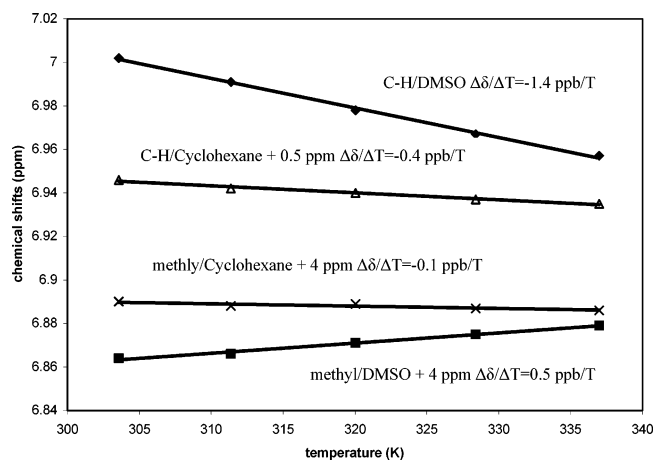


Figure 2. Temperature dependence of the proton chemical shift of *N*-methyl maleimide in DMSO-*d*₆ and cyclohexane-*d*₁₂ solutions.

chemical shifts, spectra were recorded on a VARIAN VXR 500s spectrometer at temperatures between 30 and 70 °C at 10 °C intervals.

The simplest theoretical model for hydrogen bonding between NMM and DMSO is a dimer. To explore the influence of the proton acceptor, NMM–acetone and NMM–water complexes were also studied. Molecular geometries were optimized at the B3LYP³¹/6-31G* level, which gives quite accurate structures at a relatively low cost. Binding energies between NMM and a proton acceptor molecule (D_e) were calculated at both the B3LYP and MP2 levels using 6-311G**, 6-311++G**, 6-311G-(3df,3pd), and 6-311++G(3df,3pd) basis sets. A recently developed parallel MP2 program³² was utilized in the MP2 calculations. It took 290 min to calculate the energy for the NMM–DMSO complex using the 6-311++G(3df,3pd) basis set (total 674 contracted basis functions) on four 1 GHz Pentium III processors. The basis set superposition error (BSSE) was estimated by the counterpoise method.³³ NMR shielding calculations were carried out by the gauge including atomic orbital (GIAO) approach^{34,35} at both Hartree–Fock and B3LYP levels using 6-311G** and 6-311++G** basis sets. All calculations were carried out on a Linux personal computer cluster running the PQS parallel program package.³⁶

3. Results and Discussion

Figure 2 shows the temperature dependence of the proton chemical shifts for NMM in both DMSO and cyclohexane solutions. The C–H proton chemical shifts decrease linearly with temperature in both solutions. However, in DMSO, the temperature coefficient $\Delta\delta/\Delta T$ is more than three times larger than that in cyclohexane. The difference in the temperature dependence of proton chemical shifts between the ring protons and the methyl protons is even more prominent. The chemical shift of the latter is virtually unchanged in cyclohexane solvent and slightly increases in DMSO with increasing temperature. The presence of a specific interaction between the ring protons in NMM and DMSO is also indicated by a solvent shift relative to cyclohexane solution of +0.55 ppm at 30 °C, which is much larger than normal solvent effects. By comparison, the methyl proton chemical shift changes only -0.02 ppm. The only plausible explanation for such large deshielding is the effect of a hydrogen bond. This is consistent with the polar character of the ring C(δ^-)–H(δ^+) bond in NMM, caused by neighboring electron withdrawing carbonyl groups and by sp² hybridization of the carbon atom.

Figures 3–5 show the optimized geometry for NMM–DMSO, NMM–acetone, and NMM–water complexes at the

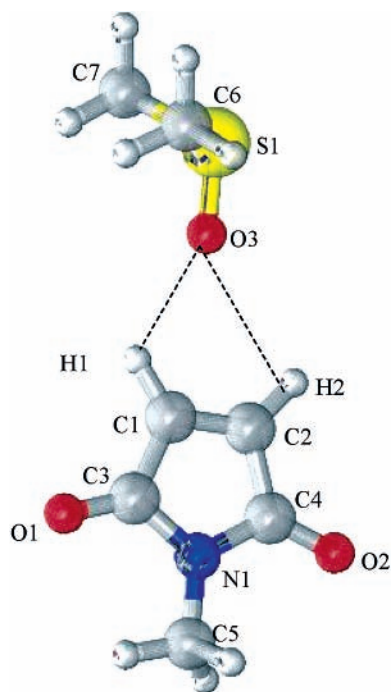


Figure 3. Optimized geometry of NMM–DMSO complex at the B3LYP/6-31G* level.

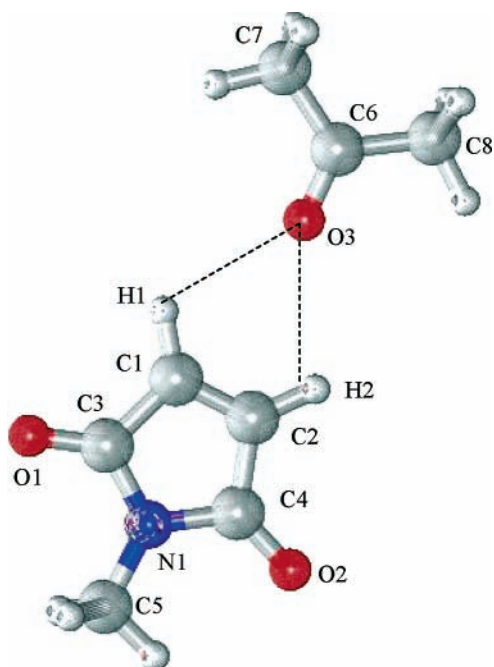


Figure 4. Optimized geometry of NMM–acetone complex at the B3LYP/6-31G* level.

B3LYP/6-31G* level. Interestingly, these complexes tend to form bifurcated hydrogen bonds, two C–H groups connecting one oxygen atom in hydrogen bond acceptors. The most important geometrical parameters for these complexes are listed in Table 1. The bond lengths of ring C–H slightly decrease upon complex formation. As mentioned in the Introduction, the shortening of C–H bonds due to hydrogen bonding is not unusual. An H···O distance less than the van der Waals contact distance, 2.7 Å,³⁷ is often taken as evidence for a C–H···O interaction. However, this weak hydrogen bond often exhibits distances in excess of that limit.³⁸ Therefore, H2···O long distances in both NMM–DMSO and NMM–H₂O complexes do not rule out the C–H···O interaction. The bond lengths

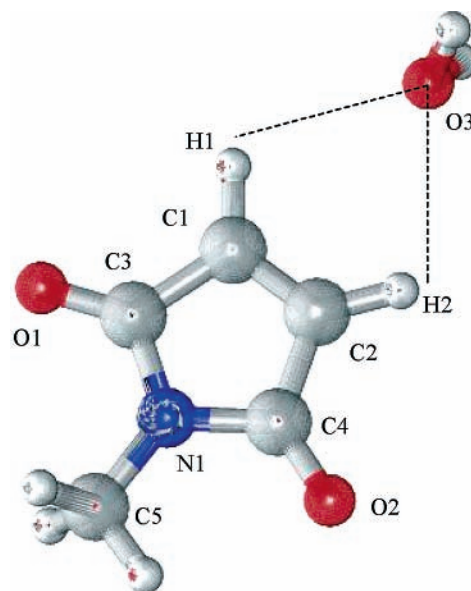


Figure 5. Optimized geometry of NMM–H₂O complex at the B3LYP/6-31G* level.

TABLE 1: Important Geometrical Parameters in NMM, NMM–DMSO, NMM–Acetone, and NMM–H₂O Complexes^a

	NMM	NMM–DMSO	NMM–acetone	NMM–H ₂ O
C–H1	1.0825	1.0815	1.8013	1.0815
C–H2	1.0825	1.0816	1.8014	1.0816
H1···O		2.417	2.609	2.669
H2···O		2.808	2.659	2.702
∠C–H1···O		119.2	112.5	112.7
∠C–H2···O		104.4	110.6	111.4
∠C–C–H1···O		1.6	0.1	–0.2

^a Distances are in Å units. Angles are in degrees.

between H1···O and H2···O, as well as the bond angles between C–H1···O and C–H2···O, are almost identical for NMM–acetone and NMM–water complexes. However, these geometrical parameters are quite different for NMM–DMSO complex. This suggests that NMM tends to form symmetric bifurcated hydrogen bonds with acetone and water and an asymmetric one with DMSO. The last row of Table 1 indicates that the proton acceptor oxygen atom lies almost in the ring plane of NMM. This coplanarity matches a criterion for attractive forces in three-center hydrogen bonds.¹⁷

The BSSE uncorrected and corrected binding energies at different theoretical levels are listed in Table 2. The B3LYP results are somewhat smaller than MP2 results and do not show a consistent trend with basis set enlargement, probably because of the inability of B3LYP to reproduce the dispersion component of the bonding.³⁹ Therefore, we concentrate on the MP2 results. The interaction energies in these complexes decrease in the order of DMSO > acetone > H₂O for all basis sets we tested. This follows the order in the basicity of the oxygen atom in these molecules. Dividing the binding energy values by the number of C–H···O interactions, we can find that the strength of the bifurcated hydrogen bond in NMM–DMSO complex is close to the upper limit of the normal range of C–H···O hydrogen bond energies. Diffuse functions are important in determining the interaction energies of weak hydrogen bonds, as shown by comparing results with different basis sets. For example, the calculated binding energies for NMM–DMSO increase 15% and 7% by including diffuse functions in 6-311G** and 6-311G-(3df,3pd) basis sets, respectively. The interaction energies obtained at the 6-311++G** basis set are even larger than those

TABLE 2: Binding Energies (kcal/mol) for NMM–DMSO, NMM–Acetone, and NMM–H₂O Complexes Before and After BSSE Correction

	NMM–DMSO		NMM–acetone		NMM–H ₂ O	
	before BSSE	after BSSE	before BSSE	after BSSE	before BSSE	after BSSE
B3LYP/6-311G**	5.10	3.33	5.50	2.19	4.09	2.29
B3LYP/6-311++G**	4.02	3.65	4.47	2.48	2.61	2.21
B3LYP/6-311G(3df,3pd)	4.77	2.93	5.56	2.21	3.63	1.80
B3LYP/6-311++G(3df,3pd)	3.19	3.14	4.37	2.37	1.90	1.89
MP2/6-311G**	6.17	3.68	6.35	2.45	4.25	2.38
MP2/6-311++G**	5.79	4.25	6.05	2.92	3.73	2.53
MP2/6-311G(3df,3pd)	6.74	4.21	7.32	3.29	4.60	2.34
MP2/6-311++G(3df,3pd)	5.28	4.51	6.26	3.51	3.13	2.76

TABLE 3: Calculated Changes in Bridging Proton Isotropic Magnetic Shieldings (in ppm) between the NMM–DMSO, NMM–Acetone, and NMM–H₂O Complexes and the Isolated NMM Molecule

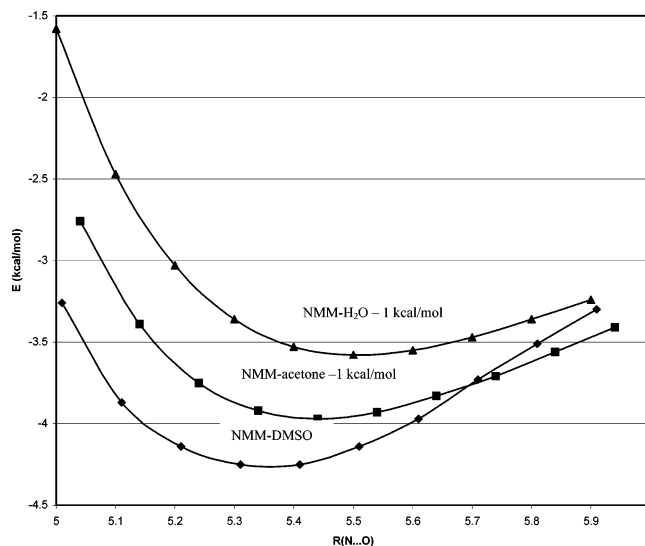
	NMM–DMSO	NMM–acetone	NMM–H ₂ O
HF/6-311G**	−0.564	−0.774	−0.441
HF/6-311++G**	−0.737	−0.890	−0.535
B3LYP/6-311G**	−0.565	−0.810	−0.452
B3LYP/6-311++G**	−0.742	−0.930	−0.581
exptl ^a	−0.556		

^a Negative difference in the chemical shift between DMSO and cyclohexane solutions

at the 6-311G(3df, 3pd) basis set for NMM–DMSO and NMM–H₂O complexes.

Calculated changes in the bridging proton isotropic shielding upon the formation of molecular complexes are listed in Table 3. We averaged the shieldings of the two protons involving the bifurcated hydrogen bonds to simulate the rapid exchange between them in experiment. We will call the change in the isotropic shielding of the bridging proton, because of the formation of the C–H···O hydrogen bond, the hydrogen bond shift. The magnitude of the hydrogen bond shift for these three bifurcated hydrogen bonded complexes is somewhat smaller than the values obtained for linear C–H···O hydrogen bonds (−1.0 ~ −1.5 ppm) at comparable theoretical levels.²⁷ Nevertheless, they exceed the threshold of 0.5 ppm suggested in an earlier work.⁴⁰ Surprisingly, the magnitudes of the calculated hydrogen bond shifts for NMM–DMSO are about 0.2 ppm smaller than that for NMM–acetone at all theoretical levels, although the former complex has stronger interaction energy. Hydrogen bond shifts become consistently more negative by about 0.11 ppm upon including diffuse functions in the basis set, in both Hartree–Fock and B3LYP calculations. From a comparison of H–F and B3LYP results, electron correlation effects are quite small for this quantity, as expected. Table 3 also shows the measured difference of the ring proton chemical shift of NMM between DMSO and cyclohexane solutions. This should roughly correspond to the hydrogen bond shift, because cyclohexane does not form hydrogen bonds. It is encouraging that the simple gas phase model reproduces the experimental value reasonably (0.74 ppm vs 0.56 ppm).

Characterizing the C–H···O hydrogen bond by its calculated properties at the static equilibrium geometry is obviously a gross simplification. The correct but very expensive procedure is to run a molecular dynamics simulation of the solute (NMM) with a large number of solvent molecules and evaluate statistical averages. Short of this, an idea of thermal averaging can be obtained from the calculated intermolecular potential curves. We have chosen the distance between the nitrogen atom in NMM and the oxygen atom in the acceptor as the independent variable. Although this distance has no physical relevance, its line bisects the bifurcated hydrogen bonds and is thus a

**Figure 6.** Change of the BSSE corrected binding energies with the $R(\text{N}\cdots\text{O})$ distance (see text) at the MP2/6-311++G** level.

convenient measure of the average hydrogen bond length. We have varied the $\text{N}\cdots\text{O}$ distance in all three complexes within the relevant range (5–6 Å) and reoptimized the geometry at each distance with the constraints that the acceptor oxygen atoms are kept on the line bisecting the two C–H···O hydrogen bonds and the orientation of the acceptor molecules is fixed. The constraints help avoid other interactions between the molecule and the solvent. The basis set superposition error (BSSE) corrected binding energy curves calculated at the MP2/6-311++G** level are shown in Figure 6. The depths of the minima reflect the strengths of the hydrogen bonds in the three complexes. However, the weaker C–H···O interactions in NMM–acetone and NMM–H₂O complexes die off more slowly with distance than does the interaction in NMM–DMSO.

Figure 7 shows that the variation of the proton magnetic shielding tensor components for NMM–DMSO and NMM–acetone complexes calculated at the B3LYP/6-311++G** level with the change of $R(\text{N}\cdots\text{O})$. Again, we averaged the values for two protons involving the bifurcated hydrogen bonds. The values of σ_{11} and σ_{22} , the perpendicular components to the hydrogen bond axis, increase with distance for both complexes. The values of σ_{33} , the parallel component, decrease in NMM–DMSO and slightly increase in NMM–acetone when two molecules are taken apart. However, the net results for both complexes are that σ_{iso} increases linearly with $\text{N}\cdots\text{O}$ separation. This confirms a previous conclusion²⁶ that the perpendicular component is deshielded by the acceptor oxygen atom and more sensitive to hydrogen bond formation. Similar results were obtained for the NMM–H₂O complex (not shown in Figure 7). The calculated trend is consistent with our experimental observations. The bridging proton chemical shifts for these

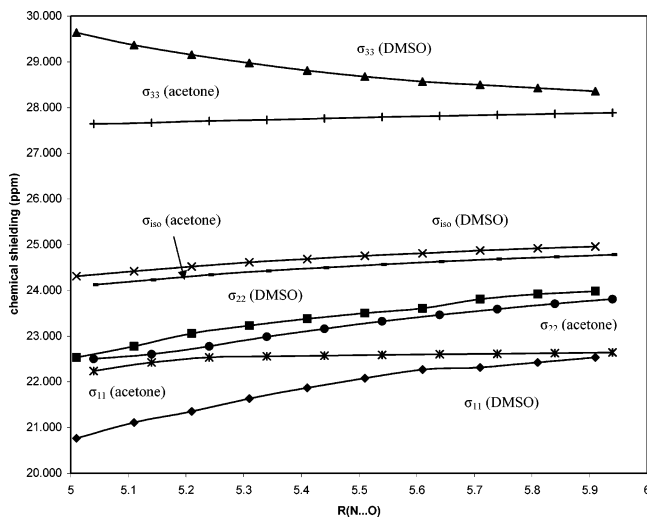


Figure 7. Change of the bridging proton isotropic shielding for NMM–DMSO and NMM–acetone complexes with the $R(N\cdots O)$ distance (see text). Shieldings were calculated at the B3LYP/6-311++G** level.

complexes depend strongly on the degree of excitation of the hydrogen bond stretching vibrational mode. As the temperature increases, more excited states are populated, which diminishes the deshielding effect due to the formation of hydrogen bonds. Therefore, the NMR shift of the bridging proton moves upfield as the temperature increases.

4. Conclusions

The C–H···O interaction between *N*-methyl maleimide and dimethyl sulfoxide was studied by measuring NMR spectra at different temperatures. The temperature coefficient, $\Delta\delta/\Delta T$, of the ring C–H proton in DMSO solution is over three times larger than that in cyclohexane solution. The sign of the temperature coefficient of the chemical shifts of the ring protons is opposite to that of the methyl protons. The ring proton chemical shift in DMSO solution is downfield shifted about 0.55 ppm compared to its value in cyclohexane solution at 30 °C. This evidence leads to the conclusion that there is a weak but well-defined C–H···O hydrogen bond between NMM and DMSO.

To characterize this interaction, theoretical calculations were carried out for three complexes: NMM–DMSO, NMM–acetone, and NMM–H₂O. Optimized geometries indicate that these complexes tend to form the bifurcated hydrogen bonds, asymmetric ones in NMM–DMSO, and symmetric ones in NMM–acetone and NMM–H₂O. BSSE corrected binding energies suggest that the order of C–H···O hydrogen bond strength is DMSO > acetone > H₂O, which follows the basicity of the acceptors. Hydrogen bond shifts (changes in the chemical shift upon hydrogen bond formation) were calculated at the Hartree–Fock and B3LYP levels. These shifts are significant although their magnitude is slightly smaller than in linear C–H···O systems. The calculated hydrogen bond shift for the NMM–DMSO complex at the optimized equilibrium position reproduces the experimental value quite well. The NMR properties in these three complexes have also been studied by scanning the $R(N\cdots O)$ distance around the equilibrium geometries. The results confirm a previous conclusion²⁶ that the perpendicular component is deshielded by the acceptor oxygen

atom and more sensitive to hydrogen bond formation than the parallel one. The isotropic shieldings for bridging protons increase linearly with the $N\cdots O$ separation, which is consistent with the experimentally obtained sign of the temperature coefficient of the chemical shift. Perhaps the most significant result of our study is that marked deviations from theoretically predicted proton chemical shifts can be used to identify weak hydrogen bonds.

Acknowledgment. We gratefully acknowledge support for this work by the National Science Foundation under Grants CHE-9707202 and CHE-0111101.

References and Notes

- (1) Green, R. D. *Hydrogen Bonding by C–H Groups*; Wiley: New York, 1974.
- (2) Steiner, T.; Saenger, W. *J. Am. Chem. Soc.* **1992**, *114*, 10146.
- (3) Gu, Y.; Kar, T.; Scheiner, S. *J. Am. Chem. Soc.* **1999**, *121*, 9411.
- (4) Allerhand, A.; Schleyer, P. v. R. *J. Am. Chem. Soc.* **1963**, *85*, 1715.
- (5) Turi, L.; Dannenberg, J. J. *J. Phys. Chem.* **1995**, *99*, 639.
- (6) Scheiner, S.; Grabowski, S. J.; Kar, T. *J. Phys. Chem. A* **2001**, *105*, 10607.
- (7) Steiner, T. *Chem. Commun.* **1997**, 727.
- (8) Muchall, H. M. *J. Phys. Chem. A* **2001**, *105*, 632.
- (9) Desiraju, G. R. *Acc. Chem. Res.* **1996**, *29*, 441.
- (10) Derewenda, Z. S.; Lee, L.; Derewenda, U. *J. Mol. Biol.* **1995**, *252*, 248.
- (11) Bella, J.; Berman, H. M. *J. Mol. Biol.* **1996**, *264*, 743.
- (12) Vargas, R.; Garza, J.; Dixon, D. A.; Hay, B. P. *J. Am. Chem. Soc.* **2000**, *122*, 4750.
- (13) Möller, C.; Plesset, M. S. *Phys. Rev.* **1934**, *46*, 618.
- (14) Dunning, T. H., Jr. *J. Chem. Phys.* **1989**, *90*, 1007.
- (15) Kendall, R. A.; Dunning, T. H., Jr.; Harrison, R. J. *J. Chem. Phys.* **1992**, *96*, 6796.
- (16) Scheiner, S.; Kar, T.; Gu, Y. *J. Biol. Chem.* **2001**, *276*, 9832.
- (17) Jeffery, G. A.; Saenger, W. *Hydrogen Bonding in Biological Structures*; Springer-Verlag: Berlin, 1991.
- (18) Hobza, P.; Spirko, V.; Havlas, Z.; Buchhold, K.; Reimann, B.; Barth, H. D.; Brutschy, B. *Chem. Phys. Lett.* **1999**, *299*, 180.
- (19) Cubero, E.; Orozco, M.; Hobza, P.; Luque, F. J. *J. Phys. Chem. A* **1999**, *103*, 6394.
- (20) Hobza, P.; Havlas, Z. *Chem. Phys. Lett.* **1999**, *303*, 447.
- (21) Scheiner, S.; Kar, T. *J. Phys. Chem. A* **2002**, *106*, 1784.
- (22) Lee, C. M.; Kumler, W. D. *J. Am. Chem. Soc.* **1962**, *84*, 571.
- (23) Mizuno, K.; Ochi, T.; Shindo, Y. *J. Chem. Phys.* **1998**, *109*, 9502.
- (24) Ash, E. L.; Sudmeier, J. L.; Day, R. M.; Vincent, M.; Torchilin, E. V.; Haddad, K. C.; Bradshaw, E. M.; Sanford, D. G.; Bachovchin, W. W. *Proc. Natl. Acad. Sci. U.S.A.* **2000**, *97*, 10371.
- (25) Rohlffing, C. M.; Allen, L. C.; Ditchfield, R. *Chem. Phys. Lett.* **1982**, *86*, 380.
- (26) Rohlffing, C. M.; Allen, L. C.; Ditchfield, R. *J. Chem. Phys.* **1983**, *79*, 4958.
- (27) Scheiner, S.; Gu, Y.; Kar, T. *J. Mol. Struct.* **2000**, *500*, 441.
- (28) Wang, B.; Hinton, J. F.; Pulay, P. *J. Comput. Chem.* **2002**, *23*, 492.
- (29) Wang, B.; Fleischer, U.; Hinton, J. F.; Pulay, P. *J. Comput. Chem.* **2001**, *22*, 1887.
- (30) Rablen, P. R.; Pearlman, S. A.; Finkbiner, J. *J. Phys. Chem. A* **1999**, *103*, 7357.
- (31) Becke, A. D. *J. Chem. Phys.* **1993**, *98*, 5648. The exact version of the B3LYP method corresponds to the implementation in the Gaussian 94 suite of programs.
- (32) Baker, J.; Pulay, P. *J. Comput. Chem.* **2002**, *23*, 1150.
- (33) Boys, S. F.; Bernardi, F. *Mol. Phys.* **1970**, *19*, 553.
- (34) Ditchfield, R. *Mol. Phys.* **1974**, *27*, 789.
- (35) Wolinski, K.; Hinton, J. F.; Pulay, P. *J. Am. Chem. Soc.* **1990**, *112*, 8251.
- (36) PQS, versions 2.3 and 2.4, Parallel Quantum Solutions. 2013 Green Acres Road, Fayetteville, Arkansas, 1999 (Web site: <http://www.pqs-chem.com>).
- (37) Taylor, R.; Kennard, O. *J. Am. Chem. Soc.* **1982**, *104*, 5063.
- (38) Desiraju, G.; Steiner, T. *The Weak Hydrogen Bond in Structural Chemistry and Biology*; Oxford University Press: Oxford, 1999.
- (39) Kristyan, S.; Pulay, P. *Chem. Phys. Lett.* **1994**, *229*, 175.
- (40) Chesnut, D. B.; Phung, C. G. *Chem. Phys.* **1990**, *91*, 147.